

HEAT CAPACITY AND PHONON SPECTRA OF $A^{III}N$

Experiment and calculation

D. Sedmidubský^{1*}, J. Leitner¹, P. Svoboda², Z. Sofer¹ and J. Macháček¹

¹Institute of Chemical Technology, Technická 5, 166 28 Prague, Czech Republic

²Faculty of Mathematics and Physics, Charles University, Ke Karlovu 5, 121 16 Prague, Czech Republic

The low temperature heat capacities of three A^{III} nitrides, A^{III} =Al, Ga and In, were measured by relaxation method in the temperature range 2–300 K and the corresponding entropies at the reference temperature 298.15 K were evaluated from the experimental data. The lattice heat capacity at constant volume was also assessed theoretically within harmonic crystal approximation by direct method using a combination of VASP software package to obtain the Hellmann-Feynman forces and the Phonon program to calculate the phonon spectra. The experimental data were analyzed by means of a Debye-Einstein model taking use of the calculated heat capacity and involving additionally an anharmonic contribution.

Keywords: *ab-initio calculations, entropy, heat capacity, nitride semiconductors, phonon, spectra*

Introduction

A^{III} nitrides (A^{III} =Al, Ga, In) with hexagonal wurtzite structure constitute a technologically important family of semiconductor materials for applications in current microelectronics and optoelectronics. Their technology is mainly based on thin films fabricated by various deposition techniques, among which MOVPE is most relevant for synthesis of high quality materials. Apart from kinetic and hydrodynamic effects, the thermodynamic stability represents a key factor for the controlled synthesis of desired materials. Hence, the accurate and reliable thermodynamic data are necessary to describe the thermodynamic behavior and to model the technological process. We have recently reported on a theoretical study of enthalpies of formation of $A^{III}N$ using *ab-initio* DFT calculations and compared the obtained results with the available experimental data [1]. In addition, based on the analysis of the available phonon spectra and some incomplete low temperature heat capacity data, we assessed the corresponding entropies [1]. However, to get more reliable values of entropies at the reference temperature we need complete sets of C_p data covering the whole temperature range 0–298 K. The low temperature heat capacities have been measured in a vacuum adiabatic calorimeter by Koshsenko *et al.* for AlN [2] and for GaN [3]. More recent data from relaxation time measurements [4] and heat flux calorimetry [5] have been also reported for GaN. To our knowledge, only the DSC heat capacities in the interval 150–300 K are available

below room temperature for the last member, InN [6]. In the present work, we combine the experimental results acquired from the relaxation time measurement with the theoretical isochoric heat capacities obtained from first principle calculations of phonon spectra.

Experimental

Powdered AlN (Alpha Alesar), GaN and InN (Sigma-Aldrich), all 99.99% purity, were compacted by uniaxial pressing at $p=300$ MPa and sintered at $T=900^\circ\text{C}$ in dynamic nitrogen atmosphere for 50 h. The phase purity of the samples prior and after the heat treatment was checked by powder X-ray diffraction (Phillips X'Pert PRO, $\text{CuK}_{\alpha 1}$ radiation). The pellets were subsequently cut into plates of typical dimensions $3\times 3\times 0.5$ mm and masses 15–25 mg suitable for heat capacity measurements.

The PPMS facility (Quantum Design) was used to acquire the heat capacity data in the temperature range of 2–320 K. It is a fully automated equipment using a hybrid adiabatic relaxation technique [7]. The PPMS software employs a two-tau relaxation method to evaluate the C_p values. Prior to each run with a given sample, a separate run with a blank holder was performed to determine the addenda associated with the sample holder and Apiezon N grease used to attach the sample. The accuracy of these heat capacity measurements is claimed not to exceed 3% [8], which was confirmed by test meas-

* Author for correspondence: David.Sedmidubsky@vscht.cz

urements on pure Cu. However, the accuracy of the measurement significantly depends on the thermal coupling between the sample and the calorimeter platform and, hence, it is expected to fall away particularly for porous samples and temperatures above ~270 K, when Apiezon tends to diffuse into the sample.

Calculation details

The phonon spectra and the corresponding heat capacities of $A^{III}N$, $A=Al$, Ga and In, were calculated within harmonic crystal approximation by means of Phonon program [9].

The Hellmann–Feynman (H–F) forces necessary to evaluate the force constants and the dynamical matrix were obtained from calculations performed by Vienna ab-initio simulation package VASP [10] within generalized gradient approximation (parametrized by PBE scheme [11]). The projector augmented wave (PAW) pseudopotentials [12] and the plane wave basis set expanded up to the cut-off energy of 532 eV were employed to treat the valence states. The first Brillouin zone was sampled within a $3\times 3\times 3$ Monkhorst-Pack k-mesh scheme. The default values of all other VASP parameters were adopted.

To generate the H–F forces, six independent atomic displacements (0.03 \AA), three for each inequivalent atom, were applied for each compound within a $2\times 2\times 2$ supercell constructed from hexagonal unit cell of the respective parent structure. Since such a supercell breaks the symmetry of the hexagonal space group ($P6_3/mmc$), the H–F forces in VASP and the force constants in Phonon had to be calculated in a rhombohedral supercell, while the further analysis of phonon frequencies was carried out in a restored hexagonal symmetry (the missing force constants were added by interpolation). In both parts of calculation, the experimentally determined lattice cell parameters (the same as those used in [1]) were considered.

Results and discussion

The A^{III} nitrides are characterized by a descending trend in bond energies when going down the A^{III} group. This has been confirmed in our recent calculations of cohesive energies and enthalpies of formation [1], which were generally in a good agreement with the experimental calorimetric data. The decreasing bond strength is consistent with the calculated H–F forces acting on the displaced atom, 355, 307 and 216 N m^{-1} obtained, respectively, for AlN, GaN and InN.

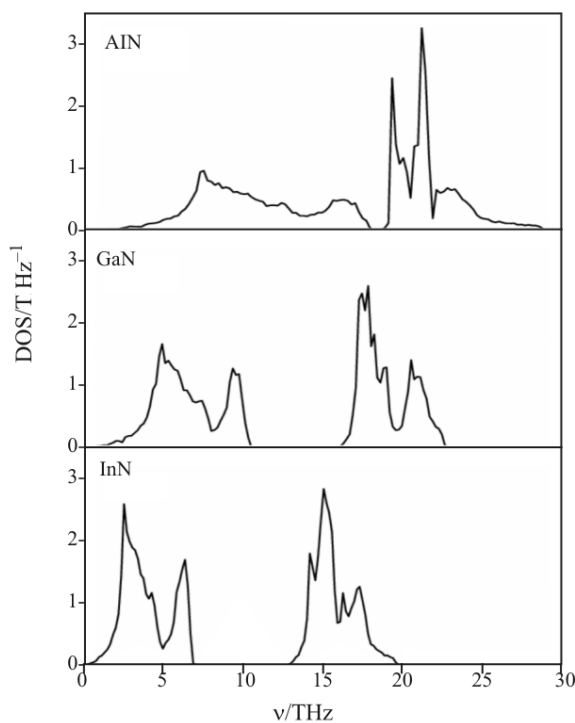


Fig. 1 Calculated phonon density of states (DOS) of AlN, GaN, InN

The resulting phonon densities of states (Fig. 1) are consistent with the decreasing H–F forces and the increasing mass of A^{III} atom. The phonon spectrum is formed by two bands separated by a gap whose width is gradually broadened and the centers of gravity of both bands move to lower frequencies on going from AlN to InN. As the lower band is predominantly contributed by A^{III} while N-vibrations mainly participate in the upper one, the proximity of the two bands in the case of AlN imposes the largest mixing compared to heavier congeners. The calculated phonon spectra are generally in a good agreement with those reported for AlN [13], GaN [14] (from time-of-flight neutron spectroscopy) and for InN [15] (from Raman scattering and IR spectroscopy), all three assessed on the basis of rigid-ion model.

The lattice heat capacities at constant volume, C_V , were directly calculated by Phonon program using the well-known relation

$$C_V = R \int_0^{\omega_{\max}} \left(\frac{\hbar\omega}{k_B T} \right)^2 \frac{e^{\hbar\omega/k_B T}}{(e^{\hbar\omega/k_B T} - 1)} g(\omega) d\omega \quad (1)$$

where g stands for phonon DOS, ω is the vibrational frequency, R gas constant, k_B Boltzmann constant and T temperature. Since all three compounds in their ideal structure are intrinsic semiconductors with well-defined band gaps, the electronic excitations do not play any role in the temperature range relevant to

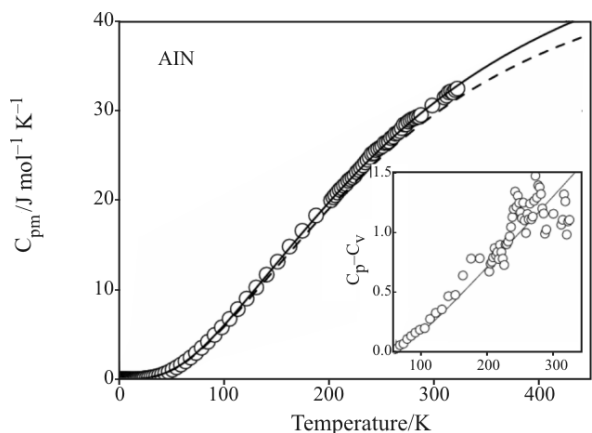


Fig. 2 Heat capacity of AlN; \circ – measured by PPMS (this work) and - - - calculated by Phonon. --- – The C_p data fitted by involving the anharmonic term in Debye–Einstein model. $C_p - C_v$ shown in the inset

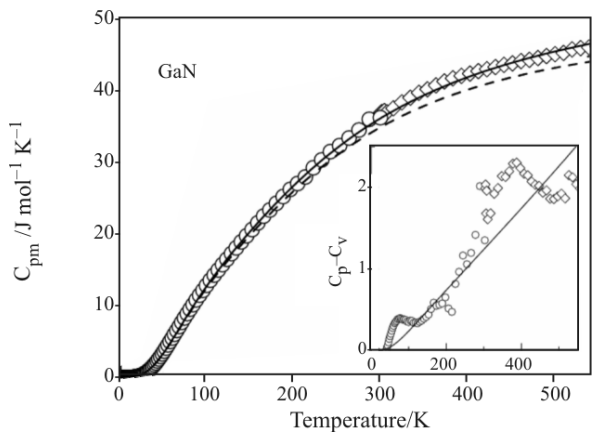


Fig. 3 Heat capacity of GaN; \circ – measured by PPMS (this work) and - - - calculated by Phonon. --- – The C_p data fitted by involving the anharmonic term in Debye–Einstein model. $C_p - C_v$ shown in the inset

this study and the lattice vibrations represent the only contribution to the heat capacity. The calculated $C_v(T)$ curves are plotted in the corresponding figures (Figs 2–4) by solid lines. As expected from the calculated phonon DOS, the saturation towards the Dulong–Petit (D–P) limit ($49.89 \text{ J mol}^{-1} \text{ K}^{-1}$) proceeds faster along the series reaching one half of D–P value at the respective temperatures 249, 187 and 144 K. Compared to the recent first-principle study performed on GaN employing ABINIT package [16, 17], our calculated curve starts to deflect to higher values at ~ 250 K and the difference amounts $\sim 3 \text{ J mol}^{-1} \text{ K}^{-1}$ at 500 K.

The experimental data acquired on PPMS are plotted in Figs. 2–4. Our previous DSC results from the interval just above the ambient temperature reported for GaN [18] and InN [19] are also showed in Figs 3 and 4 for a comparison. In all three cases the C_p data lie duly above the calculated C_v curves.

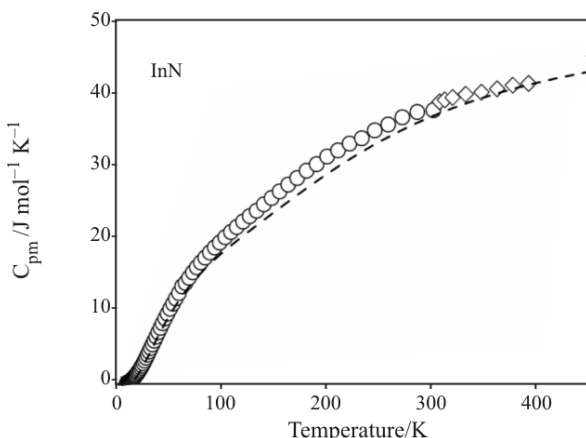


Fig. 4 Heat capacity of InN; \circ – measured by PPMS (this work) and - - - calculated by Phonon

The $C_p - C_v$ difference increases from AlN to InN and attains a nearly linear growth with temperature for AlN and GaN, while for InN it reveals an unexpected maximum at ~ 200 K, particularly when DSC data reported by Leitner *et al.* [19] are considered. It should be noted, however, that these DSC data were not fully consistent with the relative enthalpies given ibidem, the former being located slightly below the curve resulting from a simultaneous fit [19]. Nevertheless, the definite origin of the discrepancy mentioned above can be hardly identified without ambiguity.

Compared to the literature data, our AlN data are systematically diverted to higher values compared to Koshscenko *et al.* [2], which gives the difference in entropy $\sim 0.8 \text{ J mol}^{-1} \text{ K}^{-1}$ at 298 K. For GaN, on the other hand, the results of Koshscenko *et al.* [3] below 200 K lie substantially above the curves reported by Kremer *et al.* [4], Danilchenko *et al.* [5] and our data, the latter three being in nice agreement. A difference of $\sim 1.1 \text{ J mol}^{-1} \text{ K}^{-1}$ at 150 K is observed between our InN data and those of Kruckowski *et al.* [6], however, this difference falls off gradually towards room temperature.

The entropies and relative enthalpies at the reference temperature of 298.15 K were evaluated by numerical integration (trapezoidal rule) of the respective C_p/T and C_p data. The resulting values compiled in Table 1 observe linear trends with respect to A^{III} atomic number.

Table 1 Entropy S_{298}° and relative enthalpy $H_{298}^{\circ} - H_0^{\circ}$ obtained by integration of the experimental C_p data

| | $S_{298}^{\circ}/\text{J mol}^{-1} \text{ K}^{-1}$ | $H_{298}^{\circ} - H_0^{\circ}/\text{kJ mol}^{-1}$ |
|-----|--|--|
| AlN | 20.89 | 3.992 |
| GaN | 32.67 | 5.603 |
| InN | 47.82 | 7.014 |

Table 2 Characteristic temperatures Θ_D and Θ_{Ei} used in DE model to describe the lattice heat capacity within harmonic approximation and the corresponding coefficients α_D and α_{Ei} to treat the anharmonic effects

| | Θ_D | Θ_{E1} | Θ_{E2} | Θ_{E3} | α_D | α_{E1} | α_{E2} | α_{E3} |
|-----|------------|---------------|---------------|---------------|------------|---------------|---------------|---------------|
| K | | | | | | | | |
| AlN | 496 | 608 | 1025 | 1185 | 3.5 | 0 | 0 | 0 |
| GaN | 309 | 386 | 867 | 1065 | 3.3 | 1.0 | 0 | 0 |
| InN | 167 | 254 | 704 | 918 | — | — | — | — |

In order to analyze the experimental data, the $C_V(T)$ curves calculated as described above were further fitted by means of a hybrid Debye–Einstein (DE) model employing one triply degenerate Debye mode simulating three acoustic modes and three Einstein modes with the respective degeneracies 3-4-2, which approximate the remaining nine ($3n-3$, $n=4$) optical bands. Within this model the heat capacity at constant volume reads

$$C_V = R \left(\frac{3}{x_D} \right)^3 \int_0^{x_D} \frac{x^4 e^x}{(e^x - 1)^2} dx + \\ + R \sum_{i=1}^3 \frac{w_{Ei} x_{Ei} e^{x_{Ei}}}{(e^{x_{Ei}} - 1)^2} \quad (2)$$

where $x_D = \Theta_D/T$, $x_D = \Theta_{Ei}/T$ and $w_{Ei}=3, 4, 2$ are the optical mode degeneracies, which were selected with respect to the calculated phonon spectrum revealing, after subtracting the low-frequency Debye contribution, three features with the masses 3-4-2 obtained by integrating the respective parts of phonon DOS. The initial values of the characteristic temperatures Θ_{Ei} considered as free parameters for a non-linear least square refinement applied on $C_V(T)$ curves were determined as centers of gravity of the respective phonon DOS peaks. The initial guess for Θ_D was taken from the parabolic shape of low frequency phonon DOS. The resulting parameters refined with $\lambda^2 < 0.001$ and error bars less than 5 K reproduce the calculated curves quite well and are summarized in Table 2. A linearly descending trend is observed for all fitted temperatures as functions of atomic number of A^{III} .

Furthermore, a contribution to anharmonicity was considered in order to account for the difference between the experimental C_p data and C_V calculated by using harmonic crystal approximation. A correction term $(1-\alpha_i)^{-1}$ [20] was considered as a multiplication factor to each mode in the applied DE model (Eq. 2). To get the values of α_i , the characteristic temperatures were fixed at the values reproducing the C_V part and the α_i parameters were fitted on the experimental C_p data. As seen from Table 2, only one and two parameters associated with Debye and the first Einstein mode were sufficient to get a

satisfactory fit for AlN and GaN, respectively. Unfortunately, we did not succeed to achieve a reasonable fit for InN, where the $C_p - C_V$ difference first increases and then decays to zero above room temperature, which would result in unphysical negative values of some α_i . Let us note that the approach applied here for treating the anharmonicity can be considered as semi-empirical method taking into account both the anharmonic effects at constant volume and the effect of external work due to thermal expansion against external pressure. In order to model the heat capacity at constant pressure, calculations in quasi-harmonic approximation would be in place at the least.

Acknowledgements

This work was supported by the Czech Science Foundation grant No. 104/06/0642, and the Ministry of Education of CR, project No. MSM6046137302.

References

- 1 D. Sedmidubský and J. Leitner, *J. Cryst. Growth*, 286 (2006) 66.
- 2 V. I. Koshscenko, Ya. Kh. Grinberg and A. F. Demidenko, *Neorg. Mater.*, 20 (1984) 1550.
- 3 V. I. Koshscenko, A. F. Demidenko, L. D. Sabanova, V. E. Yachmenev, Yu. M. Gran and A. F. Radchenko, *Neorg. Mater.*, 15 (1979) 1686.
- 4 R. K. Kremer, M. Cardona, E. Schmidt, J. Blumm, S. K. Estreicher, M. Bockowski, M. Sanati, I. Grzegory, T. Suski and A. Jezowski, *Phys. Rev. B*, 72 (2005) 075209.
- 5 B. A. Danilchenko, T. Paszkiewicz, S. Wolski, A. Jezowski and T. Plackowski, *Appl. Phys. Lett.*, 89 (2006) 061901.
- 6 S. Krukowski, A. Witek, J. Adamczyk, J. Jun, M. Bockowski, I. Grzegory, B. Lucznik, G. Nowak, M. Wróblewski, A. Presz, S. Gierlotka, S. Stelmach, B. Palosz, S. Porowski and P. Zinn, *J. Phys. Chem. Solids*, 59 (1998) 289.
- 7 J. S. Hwang, K. T. Lin and C. Tien, *Rev. Sci. Instrum.*, 68 (1997) 94.
- 8 Quantum Design, Physical Property Measurement System – Application Note, www.qdusa.com/pdf/brochures/heat.pdf.
- 9 K. Parlinski, Software Mini-Phonon 4.28 (2007).

- 10 G. Kresse and J. Furthmüller, Phys. Rev. B, 54 (1996) 11169.
- 11 J. P. Perdew, S. Burke and M. Ernzerhof, Phys. Rev. Lett., 77 (1996) 3865.
- 12 G. Kresse and J. Joubert, Phys. Rev. B, 59 (1999) 1758.
- 13 J. C. Nipko and C.-K. Loong, Phys. Rev. B, 57 (1998) 10550.
- 14 J. C. Nipko, C.-K. Loong C. M. Balkas and R. F. Davis, Appl. Phys. Lett., 73 (1998) 34.
- 15 V. Yu. Davydov, V. V. Emtsev, I. E. Goncharuk, A. N. Smirnov, V. V. Mamutin, V. A. Vekshin, S. V. Ivanov, M. B. Smirnov and T. Inushima, Appl. Phys. Lett., 75 (1999) 3297.
- 16 H. Wang, H. Xu, T. Huang and Ch. Deng, Eur. Phys. J B, 62 (2008).
- 17 H. Wang, H. Xu, T. Huang and Ch. Deng, Eur. Phys. J B, 39 (2006) 66.
- 18 J. Leitner, A. Strejc, D. Sedmidubský and K. Ružička, Thermochim. Acta, 401 (2003) 169.
- 19 J. Leitner, P. Maršík, D. Sedmidubský and K. Ružička, J. Phys. Chem. Solids, 65 (2004) 1127.
- 20 C. A. Martin, J. Phys. Condens. Matter, 3 (1991) 5967.

DOI: 10.1007/s10973-008-9246-1